

## Organic Crystal Engineering with Piperazine–2,5–diones. 2. Crystal Packing of Weakly Dipolar Piperazinediones Derived from 2–Amino–4–bromo–7–methoxyindan–2–carboxylic Acid

Lawrence J. Williams, B. Jagadish, Michael G. Lansdown,  
Michael D. Carducci, and Eugene A. Mash\*

Department of Chemistry, The University of Arizona, Tucson, Arizona 85721–0041

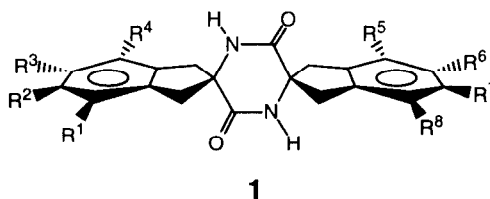
Received 9 September 1999; accepted 15 October 1999

**Abstract:** Piperazine–2,5–diones with the potential to manifest three chemically distinct and linearly independent intermolecular interactions were synthesized from the enantiomers of 2–amino–4–bromo–7–methoxyindan–2–carboxylic acid. Samples of enantiomerically pure, racemic, and meso piperazinediones were characterized in the solid state by X–ray crystallography. "Ladder–like" intermolecular amide–to–amide hydrogen bonding interactions were observed in each case, establishing tape structures parallel to one crystallographic axis. The observed tape morphologies and crystal packing closely resemble that previously observed for a topographically similar tetramethoxy–piperazinedione. The results obtained demonstrate that the weak dipoles associated with the *p*–bromoanisole moiety play no role in determining order in the crystalline state. © 1999 Elsevier Science Ltd. All rights reserved.

**Keywords:** Amino acids and derivatives, Indanes, Piperazinones, X–Ray crystal structures

### INTRODUCTION

We have initiated a program to develop molecules that participate in three independent intermolecular interactions such that they will organize in the crystalline state in a predictable fashion.<sup>1</sup> The family of piperazine–2,5–diones **1** is ideal for this purpose since conformational restriction reduces the number of possible packing modes, while structural variability permits the attachment of directed functionality to the molecular scaffold. As described in the preceding article,<sup>2</sup> six achiral molecules were prepared from 2–aminoindan–2–carboxylic acid derivatives and were characterized in the solid state by X–ray crystallography. In each case, intermolecular amide–to–amide hydrogen bonding interactions established "ladder–like" parallel tapes in the crystalline solid.<sup>3</sup> Intertape organization was dependent on the arene substitution pattern and was governed by the development of arene–arene and van der Waals contact interactions. Based on these results, we have developed a model to predict the crystal packing and interpret the crystal structures of molecules **1**.



\* Corresponding author email emash@u.arizona.edu

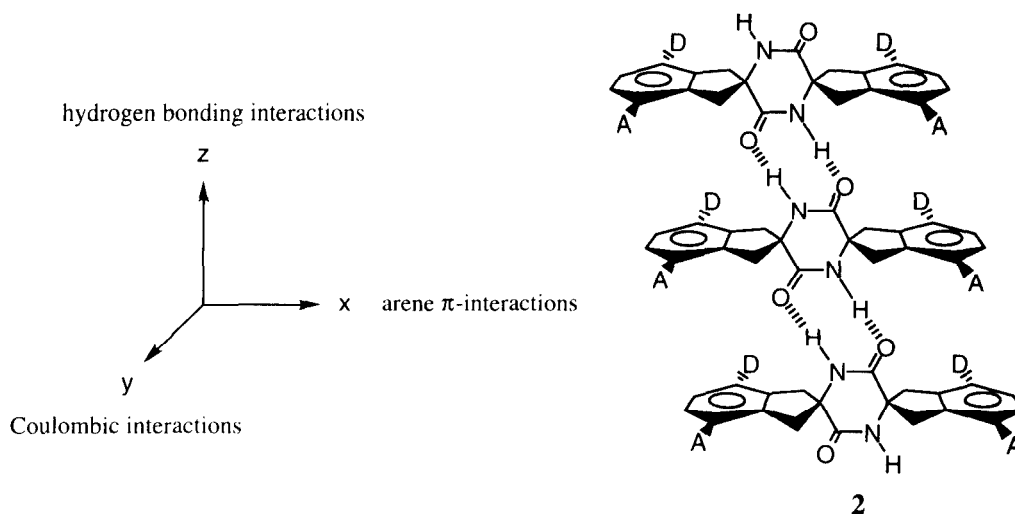
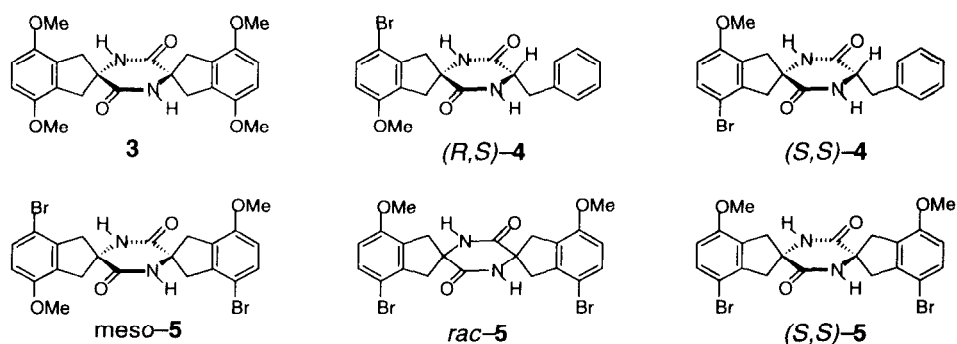


**Figure 1.** Linearly independent intermolecular interactions on a piperazinedione molecular scaffold.

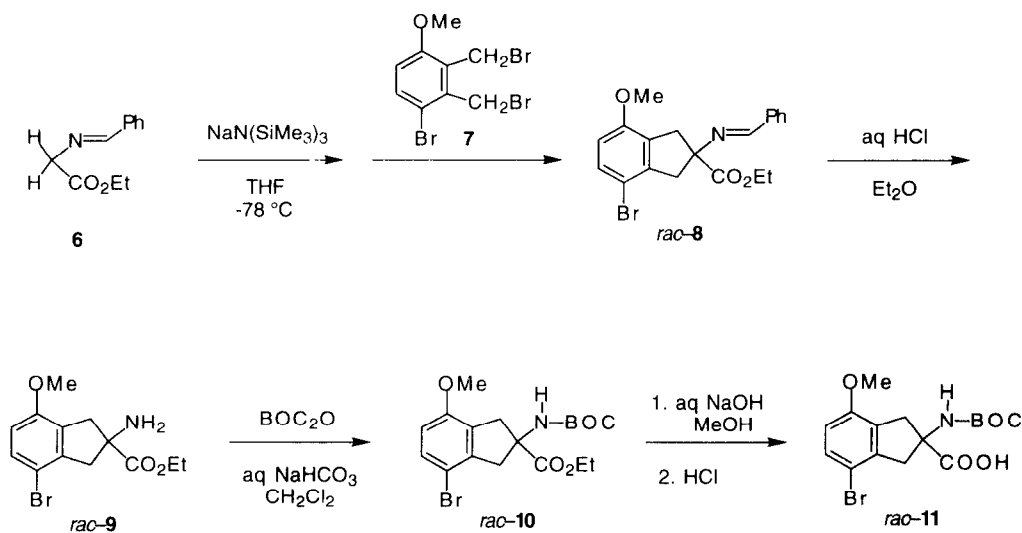
Compounds **1** were designed especially because, when enantiomerically pure as shown for **2** in Figure 1, formation of amide–to–amide hydrogen bonded tapes *requires* that the groups D reside on one side of the tape and that the groups A reside on the opposite side of the tape. Incorporation of electron donor (D) and acceptor (A) groups renders the piperazinedione molecules chiral *and* polar. Hydrogen–bonded tapes must necessarily possess aligned dipoles that are perpendicular to the tape. For sufficiently strong dipoles, Coulombic interactions might be expected to contribute to the packing forces and to determination of order in the crystalline solid.<sup>4</sup> Arene edge–to–face interactions might be expected for **2** based on the crystal structure previously obtained for achiral tetramethoxypiperazinedione **3**.<sup>2</sup> We present herein the synthesis and characterization in solution by NMR and in the solid state by X–ray crystallography of piperazinediones *meso*-**5**, *rac*-**5**, and (*S,S*)-**5**, which are topographically similar to **3** but contain the weakly dipolar *p*-bromoanisole moiety. Also presented and discussed are crystal structures of the diastereomers (*R,S*)-**4** and (*S,S*)-**4**, derived from the 2-amino-4-bromo-7-methoxyindan-2-carboxylic acid precursors to **5** and (*S*)-phenylalanine.



## RESULTS

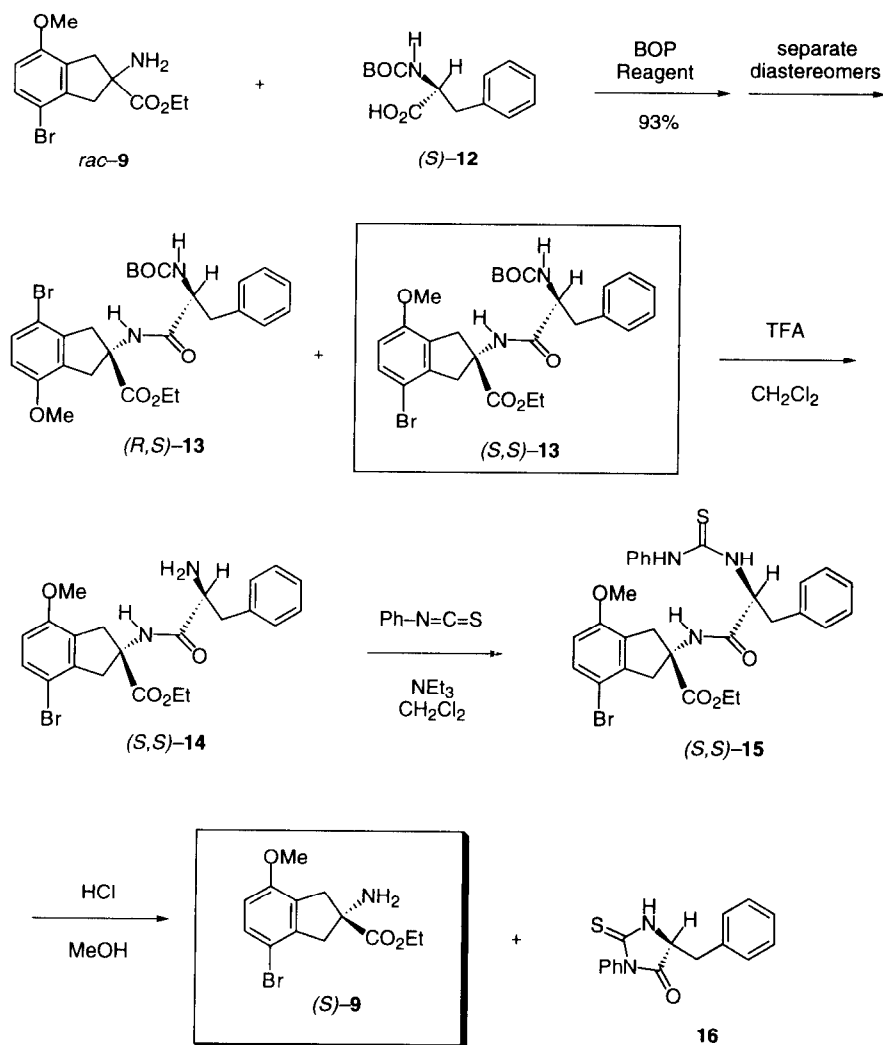
## Synthesis and Crystallization

Racemic ethyl 2-amino-4-bromo-7-methoxyindan-2-carboxylate (*rac*-**9**) and racemic 4-bromo-2-[(*N*-carbo-2,2-dimethylethoxy)amino]-7-methoxyindan-2-carboxylic acid (*rac*-**11**) were prepared as depicted in Scheme 1. Double alkylation of **6**, the benzaldehyde imine of ethyl glycinate,<sup>5</sup> with 2,3-bis(bromomethyl)-4-bromoanisole (**7**)<sup>6</sup> afforded a mixture of products which included imine *rac*-**8**.<sup>7</sup> Hydrolysis of the product mixture afforded *rac*-**9** in up to 33% yield, depending on the concentration of the reaction mixture during alkylation. The balance of starting materials **6** and **7** appeared in more polar products believed to result from intermolecular oligomerization that competes with the desired intramolecular cyclization following the first alkylation step. Treatment of *rac*-**9** with BOC anhydride produced *rac*-**10** in 83% yield. Ester hydrolysis was effected using aqueous sodium hydroxide to give *rac*-**11** in >99% yield.



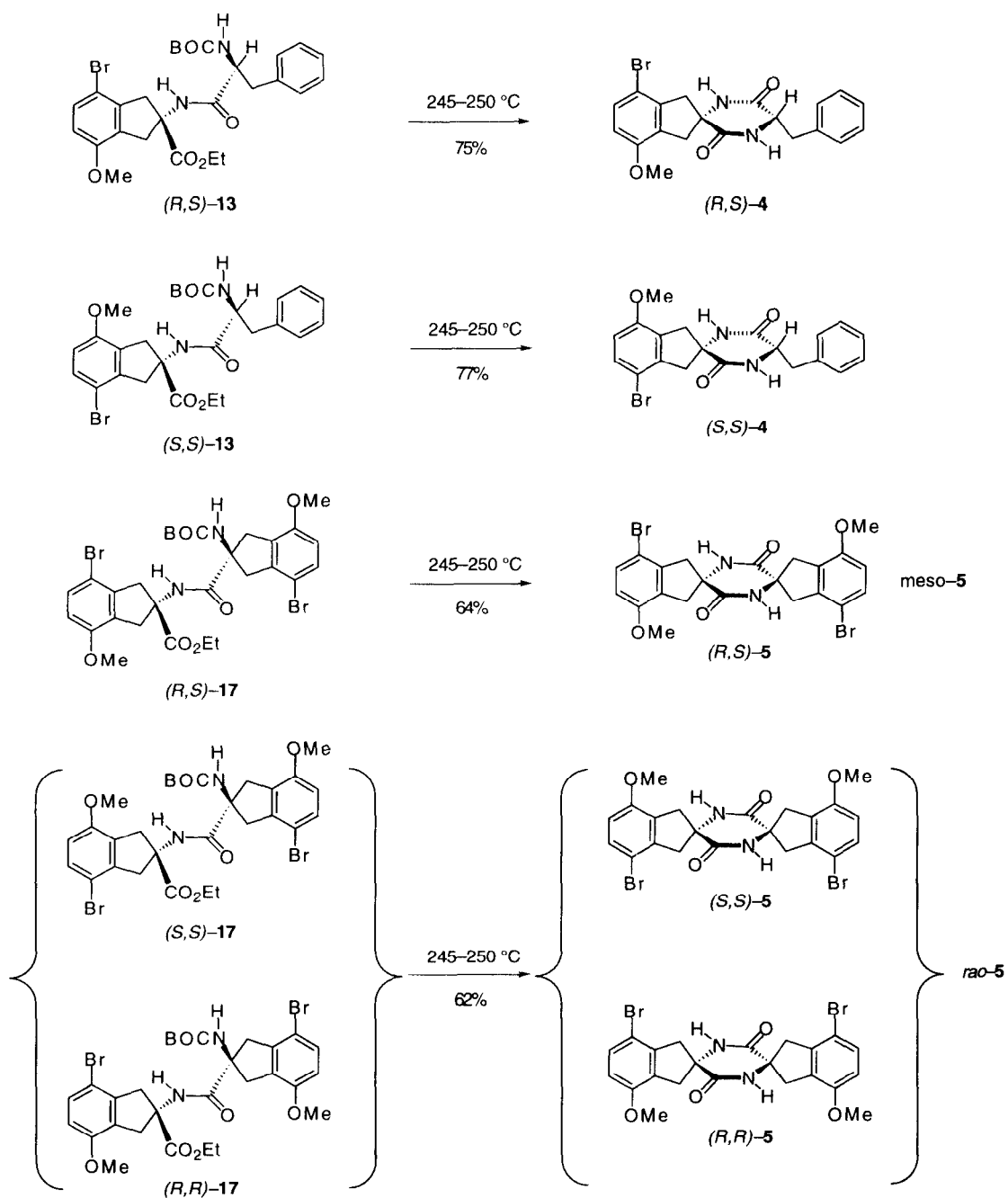
**Scheme 1.** Synthesis of (±)-Ethyl 2-Amino-4-bromo-7-methoxyindan-2-carboxylate (*rac*-**9**) and (±)-4-Bromo-2-[(*N*-carbo-2,2-dimethylethoxy)amino]-7-methoxyindan-2-carboxylic Acid (*rac*-**11**).

Coupling of *rac*-**9** with *N*-*t*-butoxycarbonyl-L-phenylalanine ((*S*)-**12**)<sup>8</sup> using benzotriazol-1-yloxy-tris(dimethylamino)phosphonium hexafluorophosphate (BOP reagent)<sup>9</sup> afforded a 1:1 mixture of dipeptides (*R,S*)-**13** and (*S,S*)-**13** in 93% yield (Scheme 2). These diastereomers were separated by gravity-driven column chromatography on silica gel 60. Structures were assigned to these diastereomers on the basis of X-ray crystallographic analyses of the corresponding piperazinediones obtained upon thermolysis (*vide infra*). Application of the Edman degradation<sup>10</sup> to (*S,S*)-**13** afforded (*S*)-**9** in >70% yield over three steps. Amino ester (*S*)-**9** was converted to (*S*)-**11** by the route previously described for the racemic compound.



**Scheme 2.** Resolution of ( $\pm$ )-Ethyl 2-Amino-4-bromo-7-methoxyindan-2-carboxylate (*rac*-9).

Coupling of (*S*)-9 with (*S*)-11 using BOP reagent gave dipeptide (*S,S*)-17 (Scheme 3) in 79% yield. Coupling of *rac*-9 with *rac*-11 afforded a 2:1:1 mixture of dipeptides (*R,S*)-17, (*R,R*)-17, and (*S,S*)-17 in 93% yield. The (*R,S*) diastereomer in this mixture was separated from the (*R,R*) and (*S,S*) enantiomers by gravity-driven column chromatography on 70–230 mesh silica gel 60 eluted with 5% ethyl acetate/benzene. Structures were assigned to the separated diastereomers by comparison of their spectroscopic and chromatographic properties with those of (*S,S*)-17 derived from (*S*)-9.



**Scheme 3.** Synthesis of Piperazinediones  $(R,S)$ -4,  $(S,S)$ -4, meso-5,  $(S,S)$ -5, and  $rac$ -5.

Table 1. Crystallographic Data for Piperazinediones 4–5.

Compound <sup>a</sup>	space group	D/pb	Z <sup>c</sup>	a (Å)	b (Å)	c (Å)	$\beta$ (deg)	$R_f^b$	$R_p^b$	$wR_2^b$	density (g/cm <sup>3</sup> )	V (Å <sup>3</sup> )	crystal habit	mp (°C)
(R,S)-4	P2 <sub>1</sub>	7.6	2	11.0646 (5)	6.0861 (3)	13.7351 (6)	94.417 (2)	0.0485	0.1210	0.1210	1.496	922.18 (7)	block	>290 (dec)
(S,S)-4	P2 <sub>1</sub>	14.4	2	11.4100 (10)	6.0950 (10)	13.475 (2)	98.930 (8)	0.0538	0.1378	0.1378	1.490	925.7 (2)	block	302–308
meso-5	P2 <sub>1</sub> /n	11.3	2	8.2817 (10)	6.1031 (10)	21.7360 (10)	97.252 (6)	0.0513	0.1446	0.1446	1.634	1089.8 (2)	rod	357–359
rac-5	P2 <sub>1</sub> /n	16.0	2	8.2961 (8)	6.1179 (6)	21.771 (2)	97.271 (2)	0.0566	0.1617	0.1617	1.625	1096.12 (18)	plate	348–351
(S,S)-5	C2	12.3	8	31.2694 (6)	6.1008 (1)	24.2676 (1)	108.928 (1)	0.0708	0.1745	0.1745	1.627	4379.2 (1)	rod	360–362

<sup>a</sup>All structures were solved using Shelx.  $R_{F_0} = \frac{\sum |F_o| - |F_c|}{\sum |F_o|}$  for  $F_o > 4\sigma(F)$  and  $wR_2 = \sqrt{\frac{\sum w(F_o^2 - F_c^2)^2}{\sum w(F_o^2)^2}}$  where  $w = \frac{1}{\sigma^2(F_o^2) + (a \times p)^2 + (b \times p)}$ .

<sup>b</sup>Data to parameter ratio. <sup>c</sup>Molecules per unit cell.

Thermolysis of dipeptides (*R,S*)-13, (*S,S*)-13, (*R,S*)-17, (*S,S*)-17, and the 1:1 mixture of (*R,R*)-17 and (*S,S*)-17 produced piperazinediones (*R,S*)-4, (*S,S*)-4, (*R,S*)-5, (*S,S*)-5, and a 1:1 mixture of the enantiomeric piperazinediones (*R,R*)-5 and (*S,S*)-5 in yields ranging from 62–77% (Scheme 3). Recrystallization of these compounds from hot, dust free solutions of dimethylsulfoxide (DMSO) by slow incremental reduction of the solution temperature in a Dewar–oil bath afforded crystals suitable for single-crystal X-ray diffraction studies. Spontaneous resolution of piperazinediones (*R,R*)-5 and (*S,S*)-5 from the racemate was not observed, as 1:1 co-crystals were obtained (*vide infra*).

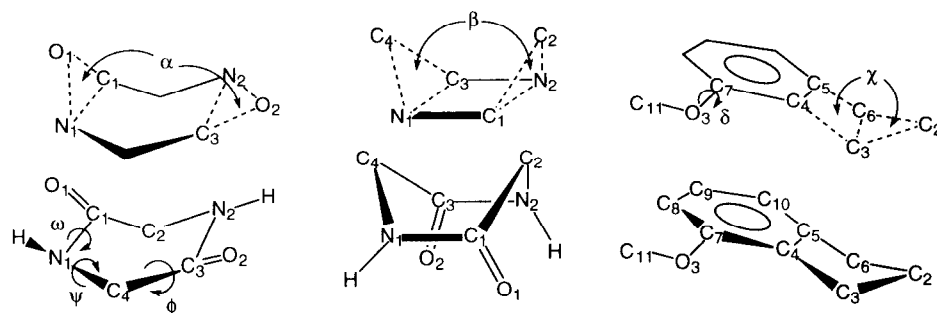
#### Crystal Structures–Molecular

Crystal structure data is given in Table 1. All compounds crystallized in monoclinic crystal systems. Geometric (conformational) data for piperazinediones 4–5 in the crystals is given in Table 2.

NMR spectra of piperazinediones 4–5 measured in DMSO-*d*<sub>6</sub> were consistent with the expected point group symmetries for these molecules in solution: *C*<sub>1</sub> for (*R,S*)-4 and (*S,S*)-4; *i* for meso-5; and *C*<sub>2</sub> for (*R,R*)-5 and (*S,S*)-5. Compounds (*R,S*)-4 and (*S,S*)-4 are nearly isostructural<sup>11</sup> and crystallized in space group *P*2<sub>1</sub>. The piperazinedione rings of (*R,S*)-4 and (*S,S*)-4 exist in shallow pseudo-twist boat conformations in the crystal ( $\alpha_{(R,S)-4} = 170^\circ$ ,  $\alpha_{(S,S)-4} = 169^\circ$ ,  $\beta_{(R,S)-4} = 159^\circ$ ,  $\beta_{(S,S)-4} = 163^\circ$ ). The indane cyclopentene rings of (*R,S*)-4 and (*S,S*)-4 are folded toward the proximal nitrogen atom of the piperazinedione ring ( $\chi_{(R,S)-4} = 143^\circ$ ,  $\chi_{(S,S)-4} = 145^\circ$ ). In both cases the phenylalanine sidechain is folded under the piperazinedione such that an intramolecular van der Waals contact occurs between the arene of the side chain and a hydrogen of the indanyl cyclopentene moiety. The arene centroid-to-hydrogen distances for this intramolecular contact are 2.84 Å for (*R,S*)-4 and 2.80 Å for (*S,S*)-4.

Compounds meso-5 and *rac*-5 are isostructural<sup>11</sup> and crystallized in space group *P*2<sub>1</sub>/*n*. The piperazinedione rings of meso-5 and *rac*-5 are very nearly planar in the crystals ( $\alpha_{\text{meso-5}} = 180^\circ$ ,  $\alpha_{\text{rac-5}} = 180^\circ$ ,  $\beta_{\text{meso-5}} = 180^\circ$ ,  $\beta_{\text{rac-5}} = 180^\circ$ ). The cyclopentene rings are symmetrically folded toward the proximal piperazinedione nitrogen ( $\chi_{\text{meso-5}} = 145^\circ$ ,  $\chi_{\text{rac-5}} = 146^\circ$ ). The torsion angles of the methoxy groups are paired ( $\delta_{\text{meso-5}} = 170^\circ$  and  $-180^\circ$  for R<sup>1</sup> and R<sup>4</sup> and  $-170^\circ$  and  $180^\circ$  for R<sup>5</sup> and R<sup>8</sup>, while  $\delta_{\text{rac-5}} = 168^\circ$  and  $180^\circ$  for R<sup>1</sup> and R<sup>4</sup> and  $-168^\circ$  and  $-180^\circ$  for R<sup>5</sup> and R<sup>8</sup>). Owing to the conformation of the piperazinedione rings, the symmetrical puckering of the cyclopentene rings, the matched methoxy group torsions, and the random and equal distribution of the bromo and methoxy substituents, apparent inversion symmetry exists for meso-5 and for *rac*-5 in the crystals.

In contrast, enantiomerically pure piperazinedione (*S,S*)-5 crystallized in space group *C*2. The asymmetric unit contained two molecules that possess different conformations. For the purpose of discussion, these conformers are labeled (*S,S*)-5a and (*S,S*)-5b. The piperazinedione rings of (*S,S*)-5a and (*S,S*)-5b in the crystal are only very slightly puckered ( $\alpha_{5a} = 177^\circ$ ,  $\beta_{5a} = 179^\circ$ ,  $\alpha_{5b} = 178^\circ$ ,  $\beta_{5b} = 179^\circ$ ). The cyclopentene rings are folded toward the proximal piperazinedione nitrogen, similarly to meso-5 and *rac*-5 ( $\chi_{5a} = 145^\circ$  and  $146^\circ$ ,  $\chi_{5b} = 146^\circ$  and  $146^\circ$ ). The methoxy groups of (*S,S*)-5a are ordered ( $\delta_{5a} = 169^\circ$  and  $170^\circ$ ), while (*S,S*)-5b bears one ordered and one disordered methoxy group ( $\delta_{5b} = 172^\circ$  and  $-180^\circ$  or  $146^\circ$ ). The conformations of the piperazinedione and cyclopentene rings and the unique methoxy group torsions eliminate the molecular two-fold rotational symmetry element from (*S,S*)-5a and (*S,S*)-5b in the crystal.

**Table 2.** Conformational Data for Piperazinediones 2–7.<sup>a</sup>

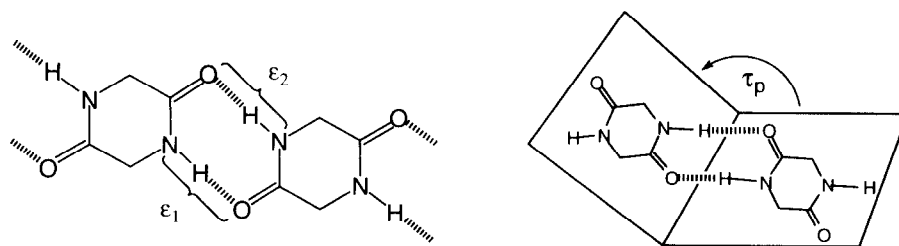
Compound	$\phi$ (deg) <sup>b</sup>	$\psi$ (deg) <sup>b</sup>	$\omega$ (deg) <sup>b</sup>	$\alpha$ (deg) <sup>c</sup>	$\beta$ (deg) <sup>c</sup>	$\chi$ (deg) <sup>d</sup>	$\delta$ (deg) <sup>e</sup>
<i>(R,S)</i> -4	-8.3	17.1	-7.7	170	159	143	-167
	-8.5	16.6	-8.3				
<i>(S,S)</i> -4	-3.8	17.4	-6.5	169	163	145	172
	-7.9	12.8	-11.4				
meso-5	-1.0	-1.1	-1.2	180	180	145	-180
	1.0	1.1	1.2				170
							180
<i>rac</i> -5							-170
	-0.9	-1.0	-1.1	180	180	146	-180
	0.9	1.0	1.1				168
							180
<i>(S,S)</i> -5a	0.7	0.6	-4.0	177	179	145	169
	2.3	2.5	-2.0			146	170
<i>(S,S)</i> -5b	0.3	1.3	-0.7	178	179	146	-180, 146 <sup>f</sup>
	1.8	-0.4	-2.4			146	172

<sup>a</sup>Values are listed for each unique substructural element. <sup>b</sup>The dihedral angles  $\phi$ ,  $\psi$ , and  $\omega$  are the torsion angles defined for conformational analysis of amide bonds in peptides.<sup>12</sup> <sup>c</sup>The dihedral angles  $\alpha$  and  $\beta$  were previously defined<sup>3b</sup> and are measures of the degree of non-planarity of the piperazinedione ring (for flat rings  $\alpha = \beta = 180^\circ$ ). <sup>d</sup>The dihedral  $\chi$  is formed by the intersection of the plane defined by C<sub>2</sub>, C<sub>3</sub>, and C<sub>6</sub> and the average plane defined by C<sub>3</sub>, C<sub>4</sub>, C<sub>5</sub>, and C<sub>6</sub> and is a measure of the degree of non-planarity of the cyclopentene ring component of the indane moiety (for flat rings  $\chi = 180^\circ$ ). <sup>e</sup>The C<sub>4</sub>-C<sub>7</sub>-O<sub>3</sub>-C<sub>11</sub> torsion angle,  $\delta$ , measures the twist of the methoxy substituent relative to the plane of the benzene ring. <sup>f</sup>Conformer *(S,S)*-5b contains a disordered methoxy group.

#### Crystal Structures—Supramolecular.

The hydrogen bonding properties of piperazinediones 4–5 were expected to play a central role in the establishment of order in the crystalline state.<sup>1–3</sup> Structural parameters germane to such hydrogen bonding networks include the N–O interatomic distances,  $\epsilon_1$  and  $\epsilon_2$ , which are indicative of the length of the N–H $\cdots$ O hydrogen bonds, and the dihedral angle from intersection of the average planes of adjacent piperazinedione rings,



**Table 3.** Intermolecular Structural Parameters for Piperazinediones 4–5: Hydrogen Bonding.<sup>a</sup>

Compound	N–O distances <sup>b</sup>		$\tau_p$ (deg) <sup>c</sup>
	$\epsilon_1$ (Å)	$\epsilon_2$ (Å)	
( <i>R,S</i> )-4	2.84	2.89	0.0
( <i>S,S</i> )-4	2.85	2.87	0.0
meso-5	2.85		0.0
rac-5	2.85		0.0
( <i>S,S</i> )-5a	2.84	2.86	0.0
( <i>S,S</i> )-5b	2.85	2.82	0.0
<b>CSD average</b>	2.89		0.0

<sup>a</sup>Values are listed for each unique substructural element. <sup>b</sup>The distance between the amide nitrogen and oxygen atoms involved in hydrogen bonding. <sup>c</sup>The dihedral  $\tau_p$  is formed by the intersection of the average planes defined by the atoms of piperazinedione rings adjacent in a tape.

$\tau_p$ . Values of these structural parameters for piperazinediones 2–7 are given in Table 3, along with average values for tape-forming piperazinediones obtained from the Cambridge Structural Database (CSD).<sup>13</sup> These data are in close agreement with the CSD averages and with data from recently published studies.<sup>1–3</sup>

Piperazinediones 4–5 form parallel "ladder-like" hydrogen-bonded tapes. Two views of molecules from the crystal structures of piperazinediones 4–5 are shown in Table 4. The column labeled "Lateral Neighbor Tapes" (LNTs) presents a view of three hydrogen-bonded tapes perpendicular to the hydrogen bonding axis. The edges of LNTs interact to form a sheet structure (*vide infra*). The column labeled "Vertical Neighbor Tapes" (VNTs) presents two pairs of "stacked" LNTs viewed down the hydrogen bonding axis. Sheets formed from LNTs have corrugated topographies that permit nesting of one sheet in another (*vide infra*).

In the case of piperazinedione (*R,S*)-4, hydrogen-bonded tapes are constructed from a single conformer. All molecules in a tape are related by translation, not by a two-fold rotation, so each edge of a tape presents a different topography. LNTs are related by screw symmetry, resulting in a "head-to-head, tail-to-tail" arrangement with indane arenes proximal to indane arenes and phenylalanine sidechains proximal to phenylalanine sidechains. The shortest distance between bromine atoms (6.09 Å) occurs for adjacent molecules in a hydrogen-bonded tape. Despite the fact that arene rings of molecules in the tape are parallel, no intratape arene face-to-face interactions occur as evidenced by the large centroid-to-centroid distances ( $\kappa_1 = 6.09$  Å, see

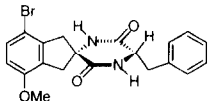
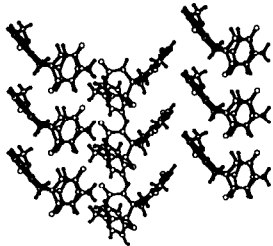
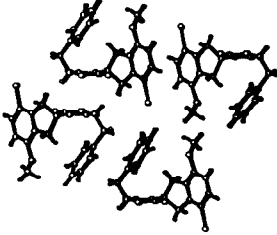
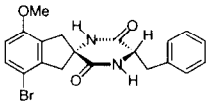
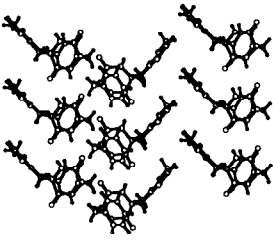
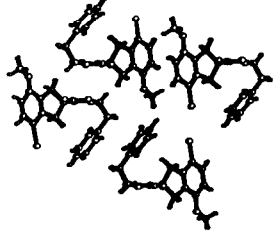
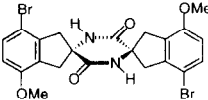
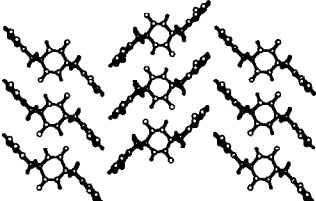
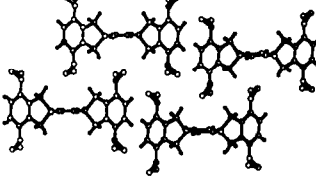
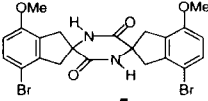
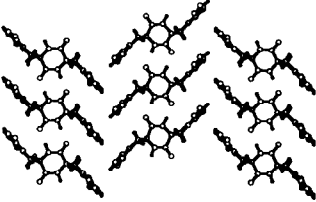
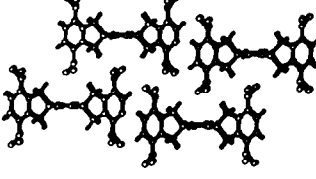
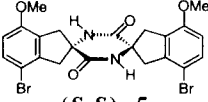
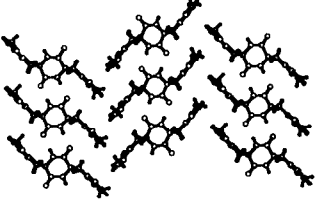
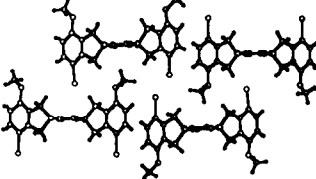
Table 5) and offset angles. The folding of the indane cyclopentene ring toward the proximal piperazinedione nitrogen serves to minimize the free volume between indane moieties of adjacent hydrogen-bonded molecules, narrowing the width and compacting the tape, and facilitates LNT interactions on one edge by more fully exposing one face of each arene. LNTs are arranged in a "herringbone" motif on the indane edge as seen in the LNT column of Table 4. The arene centroid-to-centroid distance ( $\kappa_2 = 4.84 \text{ \AA}$ ), offset angle ( $\zeta_2 = 10.6^\circ$ ), tilt angle ( $\tau_2 = 80.6^\circ$ ), and the distance from the arene centroid to the closest arene hydrogen ( $\sigma = 2.70 \text{ \AA}$ ) are consistent with arene edge-to-face interactions on the indane edge.<sup>14,15</sup> Intertape arene face-to-face and edge-to-face interactions do not occur on the phenylalanine edge as evidenced by the large centroid-to-centroid distance ( $\kappa_2 = 5.40 \text{ \AA}$ ) and offset angle ( $\zeta_2 = 40.4^\circ$ ). The phenylalanine arene centroid-to-closest hydrogen distance is  $3.32 \text{ \AA}$  and involves a side-chain hydrogen of the LNT. The "scorpion tail" folding of the phenylalanine sidechain under the piperazinedione ring is a motif previously observed in crystal packing of phenylalanine-containing piperazinediones.<sup>16</sup> This conformation produces a relatively flat surface on the phenylalanine edge of the tape so that the cross-section of two LNTs approximates a parallelogram. Sheets formed from LNTs, while relatively smooth, have a shallow corrugated topography and nest in the crystalline solid (see VNT column of Table 4).

Piperazinedione (*S,S*)-**4** is nearly isostructural<sup>11</sup> with (*R,S*)-**4** because of the similar volumes of bromine and methoxy groups.<sup>17</sup> LNTs are again related by screw symmetry, resulting in a "head-to-head, tail-to-tail" arrangement. The shortest distance between bromine atoms ( $4.24 \text{ \AA}$ ) occurs for molecules in VNTs, but is too long to represent a halogen-halogen contact interaction.<sup>4a,18</sup> Intratape and intertape arene face-to-face interactions are absent, while intertape arene edge-to-face interactions occur between indane edges of LNTs (see Table 5). The "herringbone" and "scorpion tail" motifs again produce sheets from LNTs which have a shallow corrugated topography and nest in the crystalline solid (see Table 4).

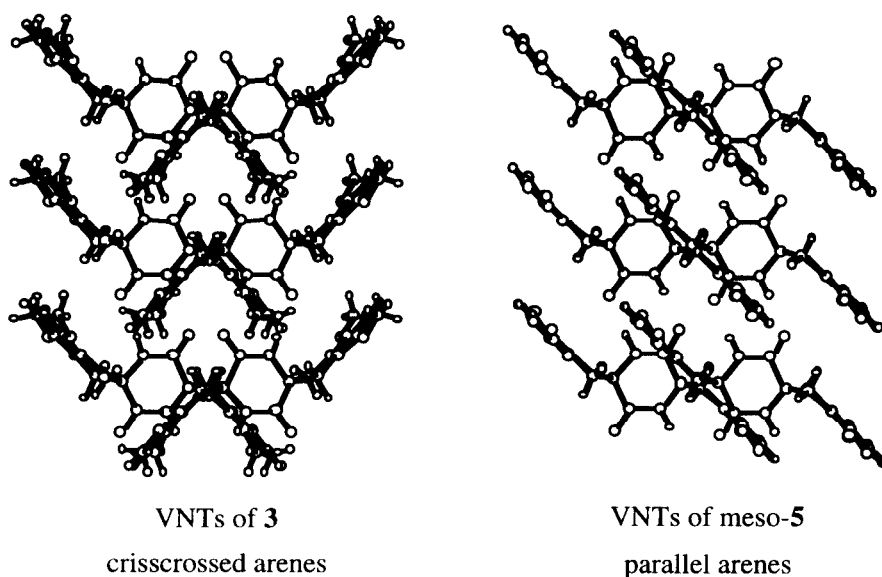
Tape morphologies for piperazinediones meso-**5**, *rac*-**5**, and (*S,S*)-**5** are similar to that previously observed for tetramethoxypiperazinedione **3**.<sup>2</sup> Meso-**5** and *rac*-**5** are isostructural<sup>11</sup> and were indistinguishable by X-ray crystallography,<sup>19</sup> and so only the crystal structure of meso-**5** will be presented and discussed here. Tapes are constructed from a single conformer of meso-**5** that possesses inversion symmetry. As was observed for **3**, arene rings of adjacent molecules of meso-**5** within a tape are parallel, but no intratape arene face-to-face interactions occur ( $\kappa_1 = 6.10 \text{ \AA}$ ,  $\zeta_1 \approx 48^\circ$ ). Symmetrical folding of the cyclopentene rings leads to a "herringbone" motif for LNTs (see Table 4). The intermolecular structural parameters for arenes of LNTs ( $\kappa_2 = 5.01 \text{ \AA}$ ,  $\zeta_2 = 17.7^\circ$ ,  $\tau_2 = 84.1^\circ$ , and  $\sigma = 2.79 \text{ \AA}$ ) are consistent with arene edge-to-face interactions. Abutment of LNTs produces sheets with a corrugated topography with one type of groove and one type of ridge. Sheets nest to maximize van der Waals contact interactions in the crystalline solid (see Table 4). However, VNTs for meso-**5** are related by translation and display a "parallel" arene alignment, whereas VNTs for **3** are related by rotation and display a "crisscrossed" arene alignment (Figure 2).

The crystal structure for (*S,S*)-**5**, while similar to **3**, meso-**5**, and *rac*-**5**, is remarkably complex. Two conformers, (*S,S*)-**5a** and (*S,S*)-**5b**, are found in the asymmetric unit. Hydrogen-bonded tapes contain only one conformer and are designated as tapes "A" and "B" for the purposes of discussion. Each edge of these tapes presents a different topography. Arene rings on adjacent molecules within a tape are parallel, but no intratape arene interactions occur ( $\kappa_1 = 6.10 \text{ \AA}$ ,  $\zeta_1 = 47.7\text{--}49.2^\circ$ ). LNTs are again arranged in a "herringbone" motif (Table 4), and the intermolecular geometric parameters ( $\kappa_2 = 4.91\text{--}5.23 \text{ \AA}$ ,  $\zeta_2 = 14.1\text{--}23.6^\circ$ ,  $\tau_2 = 83.0\text{--}83.1^\circ$ ,

**Table 4.** Lateral Neighbor Tapes and Vertical Neighbor Tapes for Piperazinediones 4–5.

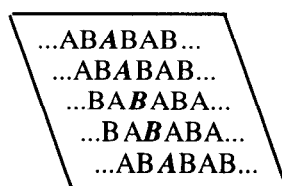
Compound	Lateral Neighbor Tapes	Vertical Neighbor Tapes
 <p><b>(<i>R,S</i>)-4</b></p>		
 <p><b>(<i>S,S</i>)-4</b></p>		
 <p><b>meso-5a</b></p>		
 <p><b>rac-5a</b></p>		
 <p><b>(<i>S,S</i>)-5</b></p>		

<sup>a</sup>The hydrogens of the methoxy substituents have been removed for clarity.

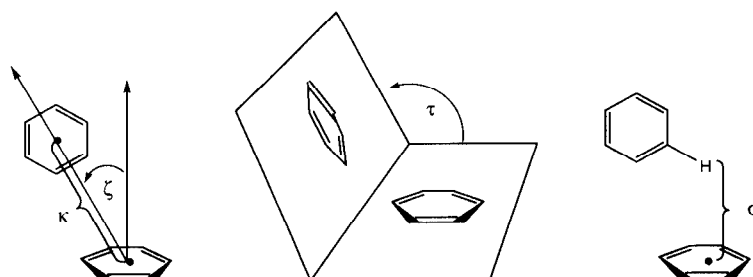


**Figure 2.** Arene crossing for vertical neighbor tapes in piperazinediones **3** and meso-**5**.

and  $\sigma = 2.75\text{--}3.02 \text{ \AA}$ ) are consistent with arene edge-to-face interactions (Table 5). Abutment of LNTs in the repeating sequence "...ABABAB..." produces sheets with a corrugated topography with four types of grooves and four types of ridges, two on each face. Sheets assemble in a pattern in which four types of VNT interactions are identifiable. These are "A over A", represented in the text by **A/A** and by bold italic letters in the schematic representation shown in Figure 3, "B over B" (**B/B**), "A over B" (**A/B**), and "B over A" (**B/A**). For **A/A** and **B/B** VNTs the associated arene rings display "crisscrossed" alignments as depicted in Figure 2, while for **A/B** and **B/A** VNTs the associated arene rings display "parallel" alignments. The closest bromine-to-bromine distance ( $3.91 \text{ \AA}$ ) occurs for **A/A** VNTs and is longer than typical Br-Br contact distances, which can be as short as  $3.20 \text{ \AA}$ .<sup>18</sup>



**Figure 3.** Schematic representation of sheets in crystalline (*S,S*)-**5**.

**Table 5.** Intermolecular Structural Parameters for Piperazinediones **4–5**: Arene Interactions.<sup>a,b</sup>

Distances and Angles between Arene Centroids <sup>c</sup>						
Compound	Within a Tape	in LNTs			in VNTs	and H <sup>d</sup>
	$\kappa_1$ (Å)	$\kappa_2$ (Å)	$\zeta_2$ (deg)	$\tau_2$ (deg)	$\kappa_3$ (Å)	$\sigma$ (Å)
<i>(R,S)</i> - <b>4</b>	6.09	4.84 <sup>e</sup>	10.6 <sup>e</sup>	80.6 <sup>e</sup>	7.89	2.70
	6.09	5.40	40.4	34.8	7.92	3.55
<i>(S,S)</i> - <b>4</b>	6.10	4.98 <sup>e</sup>	16.2 <sup>e</sup>	83.8 <sup>e</sup>	7.44	2.79
	6.10	5.43	40.6	36.2	7.78	3.48
meso- <b>5</b>	6.10	5.01	17.7	84.1	7.82	2.79
<i>rac</i> - <b>5</b>	6.11	5.01	17.6	83.7	7.81	2.79
<i>(S,S)</i> - <b>5a</b> <sup>f</sup>	6.10 <sup>h</sup>	4.91 <sup>l</sup>	15.2	83.1	7.91 <sup>k</sup>	2.75 <sup>n</sup>
	6.10 <sup>h</sup>	4.96 <sup>l</sup>	14.1	83.1	7.97 <sup>k</sup>	2.75 <sup>o</sup>
	6.10 <sup>i</sup>	5.21 <sup>j</sup>	22.9	83.0	7.90 <sup>l</sup>	2.95 <sup>o</sup>
<i>(S,S)</i> - <b>5b</b> <sup>g</sup>	6.10 <sup>i</sup>	5.23 <sup>j</sup>	23.6	83.0	7.69 <sup>m</sup>	3.02 <sup>n</sup>
					7.99 <sup>m</sup>	

<sup>a</sup>Values are listed for each unique substructural element. <sup>b</sup>For optimal face-to-face interactions,  $\kappa \approx 3.8$  Å,  $0^\circ < \zeta < 35^\circ$ , and  $\tau \approx 0^\circ$ . For optimal edge-to-face interactions,  $\kappa \approx 5.0$  Å,  $0^\circ < \zeta < 35^\circ$ , and  $\tau \approx 90^\circ$ . <sup>c</sup>Values for  $\zeta$  and  $\tau$  are listed for  $\kappa < 6.0$  Å. <sup>d</sup>Distance to the nearest arene hydrogen. <sup>e</sup>The first value refers to neighboring *p*-bromoanisoole moieties, while the second refers to neighboring phenylalanine arene moieties. <sup>f</sup>Conformer *(S,S)*-**5a** contains two ordered methoxy groups. <sup>g</sup>Conformer *(S,S)*-**5b** contains one disordered methoxy group. <sup>h</sup>Data for conformer *(S,S)*-**5a**. <sup>i</sup>Data for conformer *(S,S)*-**5b**. <sup>j</sup>For **5a/5b** lateral neighbors. <sup>k</sup>For **a x a** vertical neighbors. <sup>l</sup>For **b x b** vertical neighbors. <sup>m</sup>For **a x b** vertical neighbors. <sup>n</sup>Conformer **5a** hydrogen donor to arene of conformer **5b**. <sup>o</sup>Conformer **5b** hydrogen donor to arene of conformer **5a**.

## DISCUSSION

We postulated that predictable molecular order in crystalline solids would arise if chiral molecular building blocks were to contain three linearly independent recognition elements.<sup>1</sup> Our initial design model envisaged that piperazinediones **1**, built from enantiomerically pure derivatives of 2-aminoindan-2-carboxylic acid, would provide a suitable conformationally restricted molecular scaffold for the required recognition

elements. The first such element, amide-to-amide hydrogen bonding of the piperazinedione ring to form "ladder-like" tapes, was indeed operative in a set of prototype piperazinediones, including **3**,<sup>2</sup> as in most of the piperazinediones documented in the Cambridge Structural Database<sup>13</sup> and reported elsewhere.<sup>1–3</sup> It was anticipated that piperazinediones **4–5** would similarly form one-dimensional tapes. Based on our previous work<sup>2</sup> and the topographic homology of piperazinediones **5** with **3**,<sup>17</sup> "herringbone" motifs between LNTs were expected to lead to intermolecular arene edge-to-face interactions and the establishment of order in a second dimension perpendicular to the hydrogen-bonded tapes in the crystalline solids (see Figure 1). Incorporation of the *p*-bromoanisole moiety as the third linearly independent recognition element would serve to test the effects of weak local and net molecular dipoles on crystal packing without introducing significant topographic perturbations.

Owing to the chirality and orientation of adjacent molecules in the tapes of (*R,S*)-**4** and (*S,S*)-**4**, the dipoles due to the *p*-bromoanisole moiety were necessarily aligned in each tape.<sup>20</sup> In the case of (*S,S*)-**5**, chirality required that the dipoles due to the *p*-bromoanisole moieties be aligned on both tape edges and in the same direction (Figure 4).<sup>21</sup> For (*R,S*)-**4**, (*S,S*)-**4**, and (*S,S*)-**5** the dipoles of the *p*-bromoanisole moieties of LNTs engaged in edge-to-face interactions are opposed.

Several possibilities exist for organization of the molecules of meso-**5** and *rac*-**5** into tapes. In the case of meso-**5**, the *p*-bromoanisole dipoles might be aligned on both tape edges, but in opposite directions, or in alternate directions down each tape edge, or be randomly distributed. In the case of *rac*-**5**, spontaneous resolution would have afforded crystals like those observed for (*S,S*)-**5**. Such a resolution was not observed. In 1:1 co-crystals of (*S,S*)-**5** and (*R,R*)-**5**, the *p*-bromoanisole dipoles might still be aligned on both tape edges in the same direction if each tape was composed of one enantiomer, or could alternate in direction down a tape if the enantiomers alternate down the tape, or be randomly distributed. The best fit to the crystallographic data for crystals of meso-**5** and *rac*-**5** involved random occupancy of each of the four substitution sites (R<sup>1</sup>, R<sup>4</sup>, R<sup>5</sup>, and R<sup>8</sup>, see Figure 1) by the bromine and methoxy substituents, and so these groups appear superimposed in the crystallographic solutions. In the case of meso-**5**, this means the molecules are present in one orientation in half of the molecular positions and in an orientation related to the first by a two-fold rotation in the other half of the molecular positions, and are randomly distributed (Figure 4). For the co-crystal *rac*-**5**, the observed structure is a consequence of random occupation of the molecular positions by the enantiomers (Figure 4).

It is important to note that the crystallographic experiment is a statistical measure and cannot identify a specific molecule in a precise position in the crystal. Although the relative orientations of the dipoles of the *p*-bromoanisole moieties of LNTs engaged in edge-to-face interactions in the crystals of meso-**5** and *rac*-**5** cannot be directly determined, random occupancy of the four substitution sites requires that 50% of these dipole pairs be aligned and 50% opposed. Thus, it is concluded that the weak local and net molecular dipoles due to the *p*-bromoanisole moiety play no role in determining the crystal packing of these molecules. Instead, van der Waals interactions, approximated by topographic properties, were structure determining in directions orthogonal to the hydrogen-bonded tapes. This suggests that *all* piperazinediones topographically similar to **3** and **5** will pack similarly. Work is presently underway to test this hypothesis by replacement of the bromine and methoxy groups with other substituents to increase the dipole moment and alter the molecular topography.

Although the crystal packing of **3**, meso-**5**, *rac*-**5**, and (*S,S*)-**5** differ in the fine details, the supposition that the gross order would be maintained for these compounds proved to be correct, suggesting that the model put forth to predict the factors that determine order in these crystals was valid.

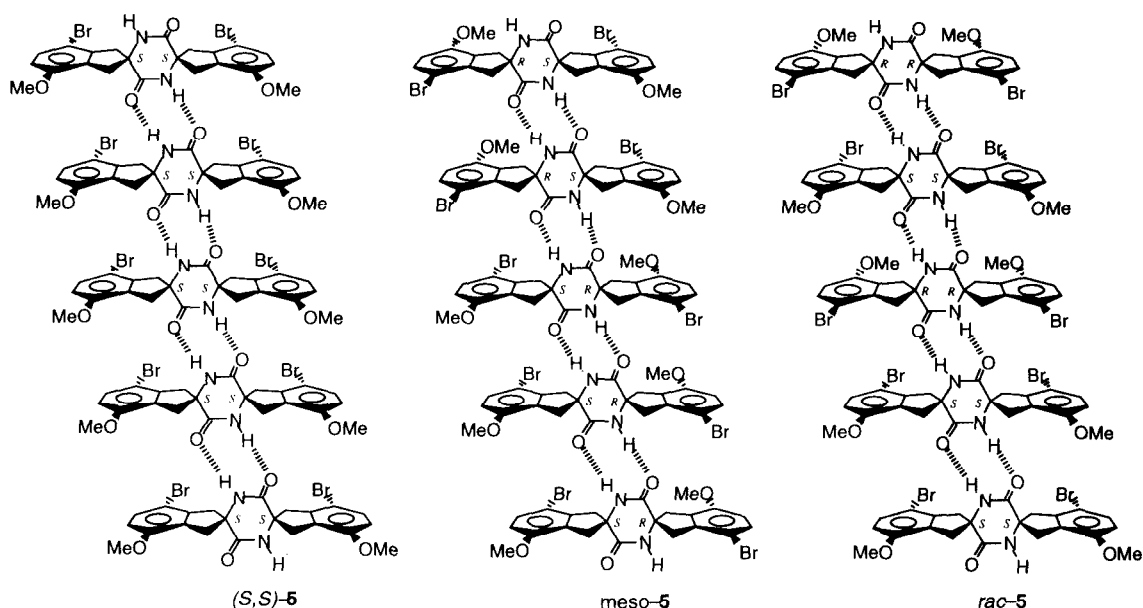


**Figure 4.** Schematic representations of tapes in crystalline  $(S,S)$ -5, meso-5, and rac-5.

## EXPERIMENTAL

### General Procedures

All reactions were performed under a positive pressure of argon. Moisture sensitive reactions were performed in glassware flame-dried under vacuum immediately before use. Reaction mixtures were stirred magnetically. Hygroscopic liquids were transferred via syringe and were introduced into reaction vessels through rubber septa. Reaction product solutions were concentrated using a rotary evaporator at 30–150 mm Hg. Dichloromethane ( $\text{CH}_2\text{Cl}_2$ ) and dimethylsulfoxide (DMSO) were distilled from  $\text{CaH}_2$ , tetrahydrofuran (THF) was distilled from sodium/benzophenone ketyl, *N,N*-dimethyl formamide (DMF) was distilled from  $\text{MgSO}_4$  under reduced pressure, and triethylamine was distilled from and stored over NaOH pellets. Analytical thin-layer chromatography was performed on Merck glass-backed, pre-coated plates (0.25 mm, silica gel 60, F-254). Visualization of spots was effected by dipping the plate in either a 2.5% solution of anisaldehyde in ethanol containing 6%  $\text{H}_2\text{SO}_4$  and 2% acetic acid or a 5% solution of phosphomolybdic acid in ethanol, followed by charring on a hot plate. Flash chromatography was performed using Merck silica gel 60 (230–400 mesh). Gravity chromatography was performed using Merck silica gel 60 (70–230 mesh). Melting points are uncorrected. Proton and  $^{13}\text{C}$  magnetic resonance spectra were recorded at 300 MHz and 75 MHz, respectively. Proton NMR spectra were referenced to tetramethylsilane (0 ppm), the residual proton signal of  $\text{CDCl}_3$  (7.24 ppm), or the center line of the residual proton signal of  $\text{DMSO}-d_6$  (2.49 ppm). Carbon NMR

spectra were referenced to the  $\text{CDCl}_3$  signal (77.0 ppm) or to the  $\text{DMSO}-d_6$  signal (39.5 ppm). Mass spectra were obtained from the Mass Spectrometry Lab in the Department of Chemistry at The University of Arizona, Tucson, Arizona. Elemental analyses were performed by Desert Analytics, Tucson, Arizona.

(±)-Ethyl 2-Amino-4-Bromo-7-methoxyindan-2-carboxylate (*rac*-9). To a solution of ethyl *N*-(phenylmethylene)glycinate<sup>5</sup> (4.80 g, 25.1 mmol) in THF (900 mL) at  $-78^\circ\text{C}$  was added NaHMDS (25.0 mL of 1.0 M solution in THF, 25 mmol) in one portion. After 45 min, 2,3-bis(bromomethyl)-4-bromoanisole<sup>6</sup> (7.50 g, 20.0 mmol) in THF (100 mL) was added in one portion. The reaction mixture was removed from the cooling bath and allowed to warm to room temperature. After 6 h, the reaction mixture was again cooled to  $-78^\circ\text{C}$  and additional NaHMDS (25 mmol) was added. The reaction mixture was removed from the cooling bath and allowed to warm to room temperature. After 6 h, the reaction was quenched by addition of brine (500 mL) followed by extraction with EtOAc (3 x 500 mL). The organic extracts were combined, dried ( $\text{MgSO}_4$ ), filtered, and concentrated to give a red oil (8.0 g). The oil was suspended in ether (500 mL) and 2 M HCl (100 mL) and the mixture was stirred vigorously. After 3 h, the layers were separated and the organic layer was washed with water (3 x 50 mL). The aqueous phase and washes were combined, the pH was adjusted to 9 with sat.  $\text{NaHCO}_3$  solution, and the solution extracted with ether (3 x 60 mL). The organic extracts were combined, dried ( $\text{MgSO}_4$ ), filtered, and concentrated to give a light yellow oil. Flash chromatography (50% EtOAc/hexanes) afforded 2.08 g (6.6 mmol, 33%) of *rac*-9,  $R_f$  0.30 (30% EtOAc/hexanes) as a clear, colorless oil that slowly solidified to a pale yellow solid, mp  $76\text{--}77^\circ\text{C}$ . IR  $\text{cm}^{-1}$  3363, 3292, 1723;  $^1\text{H}$  NMR ( $\text{CDCl}_3$ )  $\delta$  1.29 (3, t,  $J = 7.2$  Hz), 1.93 (2, s), 2.93 (1, d,  $J = 16.5$  Hz), 2.98 (1, d,  $J = 15.9$  Hz), 3.49 (1, d,  $J = 16.5$  Hz), 3.52 (1, d,  $J = 16.8$  Hz), 3.79 (3, s), 4.23 (2, q,  $J = 7.2$  Hz), 6.60 (1, d,  $J = 8.7$  Hz), 7.28 (1, d,  $J = 8.4$  Hz);  $^{13}\text{C}$  NMR ( $\text{CDCl}_3$ )  $\delta$  14.1, 44.0, 47.8, 55.3, 61.4, 63.7, 110.2, 110.5, 129.6, 130.8, 142.1, 155.4, 176.2.

Anal. Calcd for  $\text{C}_{13}\text{H}_{16}\text{BrNO}_3$ : C, 49.70; H, 5.13; N, 4.46. Found: C, 49.54; H, 5.01; N, 4.47.

(±)-4-Bromo-2-[(*N*-carbo-2,2-dimethylethoxy)amino]-7-methoxyindan-2-carboxylic Acid (*rac*-11). To a solution of *rac*-9 (1.01 g, 3.23 mmol),  $\text{NaHCO}_3$  (0.23 g) and NaCl (0.7 g) in water (7.0 mL) and  $\text{CH}_2\text{Cl}_2$  (7.0 mL) was added di-*t*-butyl dicarbonate (0.710 g, 3.23 mmol). The resultant biphasic mixture was heated to reflux. After 2 h, the mixture was cooled to room temperature, the organic layer was removed, and the aqueous layer was extracted with  $\text{CH}_2\text{Cl}_2$  (3 x 30 mL). The organic extracts were combined, dried ( $\text{MgSO}_4$ ), filtered, and concentrated to give a light yellow oil. Flash chromatography (30% EtOAc/hexanes) afforded 1.11 g (2.7 mmol, 83%) of racemic ethyl 4-bromo-2-[(*N*-carbo-2,2-dimethylethoxy)amino]-7-methoxyindan-2-carboxylate (*rac*-10),  $R_f$  0.30 (20% EtOAc/hexanes) as a white solid, mp  $161\text{--}163^\circ\text{C}$ . IR  $\text{cm}^{-1}$  3370, 2980, 1726, 1707;  $^1\text{H}$  NMR ( $\text{CDCl}_3$ )  $\delta$  1.26 (3, t,  $J = 7.2$  Hz), 1.42 (9, s), 3.27 (2, m), 3.58 (1, d,  $J = 17.1$  Hz), 3.60 (1, d,  $J = 17.1$  Hz), 3.79 (3, s), 4.22 (2, q,  $J = 7.2$  Hz), 5.13 (1, s), 6.59 (1, d,  $J = 8.7$  Hz), 7.28 (1, d,  $J = 8.9$  Hz);  $^{13}\text{C}$  NMR ( $\text{CDCl}_3$ )  $\delta$  14.1, 28.2, 42.0, 45.7, 55.3, 61.7, 64.5, 80.0, 109.7, 110.5, 129.1, 130.9, 141.6, 154.7, 155.1, 173.2.

Anal. Calcd for  $\text{C}_{18}\text{H}_{24}\text{BrNO}_5$ : C, 52.18; H, 5.84; N, 3.38. Found: C, 51.84; H, 5.73; N, 3.58.

To a solution of *rac*-10 (1.30 g, 2.85 mmol) in water (12 mL) and ethanol (70 mL) was added 2 M NaOH (7.1 mL, 14.2 mmol). After stirring at room temperature for 24 h, the solution was concentrated to ca. 5 mL, diluted with water (5 mL), and treated with 2 M HCl to produce a solution acidic by pH paper. The



aqueous mixture was extracted with ether (3 x 30 mL). The organic extracts were combined, dried (MgSO<sub>4</sub>), filtered, and concentrated to give 1.19 g (2.85 mmol, 100%) of *rac*-**11**, homogeneous by TLC, R<sub>f</sub> 0.65 (16% ethanol/CHCl<sub>3</sub>), as a white solid, mp >253 °C (dec). IR cm<sup>-1</sup> 3334, 2973, 1724, 1655; <sup>1</sup>H NMR (DMSO-*d*<sub>6</sub>) δ 1.36 (9, s), 3.17 (2, m), 3.39 (2, m), 3.74 (3, s), 6.76 (1, d, J = 8.7 Hz), 7.32 (1, d, J = 8.7 Hz), 7.57 (1, s); <sup>13</sup>C NMR (DMSO-*d*<sub>6</sub>) δ 28.1, 41.0, 44.8, 55.4, 63.6, 78.2, 108.9, 111.2, 129.3, 130.6, 141.8, 154.8, 155.2, 174.9.

Anal. Calcd for C<sub>16</sub>H<sub>20</sub>BrNO<sub>5</sub>: C, 49.75; H, 5.22; N, 3.63. Found: C, 49.71; H, 5.07; N, 3.56.

*(R,S)*-N-[4-Bromo-2-(carboethoxy)-7-methoxyindan-2-yl]-2-[(N-carbo-2,2-dimethylethoxy)amino]-3-phenylpropanamide [(*R,S*)-**13**] and *(S,S)*-N-[4-Bromo-2-(carboethoxy)-7-methoxyindan-2-yl]-2-[(N-carbo-2,2-dimethylethoxy)amino]-3-phenylpropanamide [(*S,S*)-**13**]. To a solution of *rac*-**9** (3.40 g, 10.1 mmol), L-*N*-BOC phenylalanine<sup>8</sup> (4.00 g, 15.1 mmol), and triethylamine (2.28 mL) in DMF (50 mL) was added BOP reagent<sup>9</sup> (6.80 g, 15.1 mmol). After stirring at room temperature for 2 h, the solution was diluted with EtOAc (400 mL) and water (200 mL). The organic layer was removed and the aqueous layer was extracted with EtOAc (2 x 400 mL). The organic extracts were combined and sequentially washed with 2 M HCl (3 x 400 mL), water (400 mL), saturated NaHCO<sub>3</sub> (2 x 400 mL), water (400 mL), then dried (MgSO<sub>4</sub>), filtered, and concentrated to give a light yellow oil. Flash chromatography (20% EtOAc/benzene) afforded 5.29 g (9.3 mmol, 93%) of a mixture of *(R,S)*-**13** and *(S,S)*-**13**, R<sub>f</sub> 0.62 (20% EtOAc/benzene) as a white solid. Gravity column chromatography (5% EtOAc/benzene) achieved separation of *(R,S)*-**13**, mp 192–193 °C, R<sub>f</sub> 0.34, from *(S,S)*-**13**, R<sub>f</sub> 0.27 (5% EtOAc/benzene), mp 151–152 °C. Spectral data for *(R,S)*-**13**: [α]<sub>D</sub><sup>23</sup> -15.0 (c 1.00, CHCl<sub>3</sub>); IR cm<sup>-1</sup> 3350, 3260, 1741, 1686; <sup>1</sup>H NMR (CDCl<sub>3</sub>) δ 1.23 (3, t, J = 7.2 Hz), 1.37 (9, s), 3.00–3.09 (3, m), 3.22 (1, d, J = 17.4 Hz), 3.57 (1, d, J = 17.1 Hz), 3.59 (1, d, J = 17.1 Hz), 3.78 (3, s), 4.20 (2, q, J = 7.2 Hz), 4.31 (1, m), 5.10 (1, br s), 6.53 (1, s), 6.59 (1, d, J = 8.7 Hz), 7.16–7.29 (6, m); <sup>13</sup>C NMR (CDCl<sub>3</sub>) δ 14.0, 28.1, 38.2, 41.6, 45.4, 55.3, 61.8, 64.1, 80.1, 109.6, 110.5, 126.8, 128.6, 129.1, 129.3, 131.0, 136.5, 141.3, 155.0, 155.3, 170.8, 172.3.

Anal. Calcd for C<sub>27</sub>H<sub>33</sub>BrN<sub>2</sub>O<sub>6</sub>: C, 57.76; H, 5.92; N, 4.99. Found: C, 57.47; H, 6.00; N, 4.97.

Spectral data for *(S,S)*-**13**: [α]<sub>D</sub><sup>23</sup> -3.7 (c 0.54, CHCl<sub>3</sub>); IR cm<sup>-1</sup> 3341, 3265, 1740, 1682; <sup>1</sup>H NMR (CDCl<sub>3</sub>) δ 1.23 (3, t, J = 7.2 Hz), 1.37 (9, s), 3.02 (2, m), 3.16 (1, d, J = 16.8 Hz), 3.47 (1, d, J = 17.1 Hz), 3.53–3.65 (2, m), 3.77 (3, s), 4.20 (2, q, J = 7.2 Hz), 4.30 (1, br s), 5.12 (1, br s), 6.40 (1, s), 6.58 (1, d, J = 8.4 Hz), 7.16–7.30 (6, m); <sup>13</sup>C NMR (CDCl<sub>3</sub>) δ 14.0, 28.1, 38.4, 41.9, 45.1, 55.3, 61.8, 64.1, 80.1, 109.7, 110.5, 110.5, 126.8, 128.6, 129.2, 129.3, 131.0, 136.5, 141.7, 155.0, 170.7, 172.2.

Anal. Calcd for C<sub>27</sub>H<sub>33</sub>BrN<sub>2</sub>O<sub>6</sub>: C, 57.76; H, 5.92; N, 4.99. Found: C, 57.69; H, 5.88; N, 5.06.

*Thiourea* (*S,S*)-**15**. To a solution of *(S,S)*-**13** (1.65 g, 2.94 mmol) in CH<sub>2</sub>Cl<sub>2</sub> (20 mL) was added TFA (20 mL). After 1 h at room temperature, the mixture was made basic to pH paper by addition of NaOH (2 M) and was extracted with diethyl ether (3 x 75 mL). The organic extracts were combined, dried (MgSO<sub>4</sub>), filtered, and concentrated to give *(S,S)*-**14** as a light yellow oil (1.42 g) homogeneous by TLC, R<sub>f</sub> 0.20 (80% EtOAc/hexanes). This oil was dissolved in a solution of CH<sub>2</sub>Cl<sub>2</sub> (21 mL), triethylamine (375 μL), and phenylisothiocyanate (1.13 mL, 9.40 mmol). After 16 h at room temperature, the mixture was concentrated to give a light yellow oil. Flash chromatography (30% EtOAc/hexanes) afforded 1.25 g (2.10 mmol, 71%) of *(S,S)*-**15**, R<sub>f</sub> 0.25 (30% EtOAc/hexanes) as a white solid, mp 115–117 °C (dec). [α]<sub>D</sub><sup>23</sup> -12.0 (c 3.76, CDCl<sub>3</sub>);

IR  $\text{cm}^{-1}$  3327, 1720, 1675, 1518;  $^1\text{H}$  NMR ( $\text{CDCl}_3$ )  $\delta$  1.20 (3, t,  $J = 7.0$  Hz), 2.94 (1, dd,  $J = 13.5$  Hz, 8.8 Hz), 3.10 (1, d,  $J = 17.4$  Hz), 3.12 (1, d,  $J = 17.4$  Hz), 3.34 (1, dd,  $J = 13.5$  Hz, 6.0 Hz), 3.44 (1, d,  $J = 17.4$  Hz), 3.57 (1, d,  $J = 17.1$  Hz), 3.76 (3, s), 5.16 (1, m), 6.31 (1, s), 6.59 (1, d,  $J = 8.4$  Hz), 6.88 (1, d,  $J = 7.2$  Hz), 7.06 (2, d,  $J = 7.8$  Hz), 7.18–7.39 (9, m), 7.93 (1, s);  $^{13}\text{C}$  NMR ( $\text{CDCl}_3$ )  $\delta$  14.0, 38.1, 41.8, 45.0, 55.3, 59.3, 61.8, 64.3, 109.7, 110.6, 124.7, 127.0, 127.2, 128.5, 128.6, 129.2, 130.1, 131.1, 135.7, 136.3, 141.4, 155.0, 169.9, 171.9, 179.5.

Anal. Calcd for  $\text{C}_{29}\text{H}_{30}\text{BrN}_3\text{O}_4\text{S}$ : C, 58.39; H, 5.07; N, 7.04. Found: C, 58.44; H, 5.04; N, 6.91.

*(S)*-Ethyl 2-Amino-4-Bromo-7-methoxyindan-2-carboxylate (*(S)*-9). A solution of *(S,S)*-15 (1.12 g, 1.87 mmol) in trifluoroacetic acid (15 mL) was heated to reflux for 30 min. Volatiles were then removed in vacuo, the residue taken up in 2 N HCl (50 mL), and the solution extracted with hexanes (3 x 30 mL). The aqueous phase was made basic to pH paper by addition of  $\text{NaHCO}_3$  and extracted with ether (3 x 50 mL). The organic extracts were combined, dried ( $\text{MgSO}_4$ ), filtered, and concentrated to give 556 mg (1.77 mmol, 94%) of *(S)*-9 as a clear colorless oil,  $[\alpha]_{\text{D}}^{23} -1.35$  ( $c$  12.9,  $\text{CDCl}_3$ ), which was otherwise identical to racemic *rac*-9.

*(S)*-4-Bromo-2-[(*N*-carbo-2,2-dimethylethoxy)amino]-7-methoxyindan-2-carboxylic Acid (*(S)*-11). To a solution of *(S)*-9 (1.01 g, 3.23 mmol),  $\text{NaHCO}_3$  (0.23 g), and NaCl (0.7 g) in water (7.0 mL) and  $\text{CH}_2\text{Cl}_2$  (7.0 mL) was added di-*t*-butyl dicarbonate (0.71 g, 3.23 mmol). The resultant biphasic mixture was heated to reflux. After 2 h, the mixture was cooled to room temperature, the organic layer was removed, and the aqueous layer was extracted with  $\text{CHCl}_3$  (3 x 30 mL). The organic extracts were combined, dried ( $\text{MgSO}_4$ ), filtered, and concentrated to give a light yellow oil. Flash chromatography (30% EtOAc/hexanes) afforded 1.11 g (2.7 mmol, 83%) of *(S)*-ethyl 4-bromo-2-[(*N*-carbo-2,2-dimethylethoxy)amino]-7-methoxyindan-2-carboxylate, *(S)*-10,  $R_f$  0.30 (20% EtOAc/hexanes), as a white solid, mp 161–163 °C,  $[\alpha]_{\text{D}}^{23} +2.7$  ( $c$  1.81,  $\text{CDCl}_3$ ), which was otherwise identical to racemic *rac*-10.

Anal. Calcd for  $\text{C}_{18}\text{H}_{24}\text{BrNO}_5$ : C, 52.18; H, 5.84; N, 3.38. Found: C, 51.90; H, 5.86; N, 3.32.

To a solution of *(S)*-10 (1.30 g, 2.85 mmol) in water (12 mL) and ethanol (70 mL) was added 2 M NaOH (7.1 mL, 14.2 mmol). After stirring at room temperature for 24 h, the solution was concentrated to 5 mL, diluted with water (5 mL), and treated with 2 M HCl to produce a solution acidic by pH paper. The aqueous mixture was extracted with ether (3 x 30 mL). The organic extracts were combined, dried ( $\text{MgSO}_4$ ), filtered, and concentrated to give 1.19 g (2.85 mmol, 100%) of *(S)*-11 homogeneous by TLC,  $R_f$  0.65 (16% ethanol/ $\text{CHCl}_3$ ), as a white solid, mp >253 °C (dec),  $[\alpha]_{\text{D}}^{23} -5.9$  ( $c$  1.00, MeOH), which was otherwise identical to racemic *rac*-11.

Anal. Calcd for  $\text{C}_{16}\text{H}_{20}\text{BrNO}_5$ : C, 49.75; H, 5.22; N, 3.63. Found: C, 49.64; H, 5.14; N, 3.76.

*(R,S)*-*N*-[4-Bromo-2-(carboethoxy)-7-methoxyindan-2-yl]-4-bromo-2-[(*N*-carbo-2,2-dimethylethoxy)-amino]-7-methoxyindan-2-carboxamide [*(R,S)*-17] and a Mixture of *(S,S)*-*N*-[4-Bromo-2-(carboethoxy)-7-methoxyindan-2-yl]-4-bromo-2-[(*N*-carbo-2,2-dimethylethoxy)amino]-7-methoxyindan-2-carboxamide [*(S,S)*-17] and *(R,R)*-*N*-[4-Bromo-2-(carboethoxy)-7-methoxyindan-2-yl]-4-bromo-2-[(*N*-carbo-2,2-dimethylethoxy)amino]-7-methoxyindan-2-carboxamide [*(R,R)*-17]. To a solution of *rac*-9 (1.60 g, 5.10 mmol), *rac*-11 (1.19 g, 3.09 mmol), and triethylamine (1.4 mL) in DMF (15 mL) was added BOP reagent<sup>9</sup>

(1.37 g, 3.1 mmol). After stirring at room temperature for 24 h, the solution was diluted with EtOAc (150 mL) and water (100 mL). The organic layer was removed and the aqueous layer was extracted with EtOAc (2 x 150 mL). The organic extracts were combined and sequentially washed with 3 M HCl (3 x 150 mL), water (150 mL), 2 M NaOH (2 x 150 mL), water (150 mL), then dried (MgSO<sub>4</sub>), filtered, and concentrated to give a light yellow solid. Flash chromatography (20% EtOAc/benzene) afforded 1.97 g (2.9 mmol, 93%) of a mixture of (*S,S*)-**17**, (*R,R*)-**17**, R<sub>f</sub> 0.66 (20% EtOAc/benzene), and (*R,S*)-**17**, R<sub>f</sub> 0.61 (20% EtOAc/benzene), as a white solid, and 0.55 g of unreacted *rac*-**9**. Gravity column chromatography (5% EtOAc/benzene) achieved separation of a mixture of (*S,S*)-**17** and (*R,R*)-**17**, R<sub>f</sub> 0.40 (5% EtOAc/benzene), mp 204–206 °C, from (*R,S*)-**17**, R<sub>f</sub> 0.28, mp 206–208 °C. Spectral data for the mixture of (*S,S*)-**17** and (*R,R*)-**17**: IR cm<sup>-1</sup> 3430, 3294, 1733, 1704, 1677; <sup>1</sup>H NMR (DMSO-*d*<sub>6</sub>) δ 1.04 (3, t, J = 6.9 Hz), 1.15 (9, s), 3.03 (1, d, J = 16.8 Hz), 3.06 (1, d, J = 16.2 Hz), 3.33–3.53 (6, m), 3.74 (6, s), 3.98 (2, q, J = 6.9 Hz), 6.75 (2, d, J = 8.4 Hz), 7.23 (1, s), 7.30 (2, d, J = 8.4 Hz), 8.45 (1, s); <sup>13</sup>C NMR (DMSO-*d*<sub>6</sub>) δ 13.7, 27.7, 40.6, 44.3, 55.3, 55.3, 60.6, 63.6, 64.1, 78.3, 109.0, 111.0, 129.1, 129.7, 130.4, 130.6, 141.3, 141.7, 154.5, 154.9, 172.7, 173.0; HRMS (FAB<sup>+</sup>) calcd for C<sub>29</sub>H<sub>34</sub>Br<sub>2</sub>N<sub>2</sub>O<sub>7</sub> 683.0793, found 683.0780.

Spectral data for (*R,S*)-**17**: IR cm<sup>-1</sup> 3432, 3297, 1732, 1708, 1678; <sup>1</sup>H NMR (DMSO-*d*<sub>6</sub>) δ 1.03 (3, t, J = 7.2 Hz), 1.14 (9, s), 3.04 (2, m), 3.26–3.60 (6, m), 3.75 (6, m), 3.98 (2, q, J = 7.2 Hz), 6.75 (2, d, J = 8.4 Hz), 7.22 (1, s), 7.31 (2, d, J = 8.4 Hz), 8.45 (1, s); <sup>13</sup>C NMR (DMSO-*d*<sub>6</sub>) δ 13.7, 27.7, 40.7, 44.3, 55.3, 55.3, 60.6, 63.6, 64.0, 78.3, 109.0, 109.1, 111.0, 128.2, 128.8, 129.3, 130.4, 130.6, 141.6, 142.0, 154.5, 154.8, 172.7, 173.1.

Anal. Calcd for C<sub>29</sub>H<sub>34</sub>Br<sub>2</sub>N<sub>2</sub>O<sub>7</sub>: C, 51.04; H, 5.02; N, 4.11. Found: C, 51.18; H, 4.84; N, 4.17.

(*S,S*)-N-[4-Bromo-2-(carboethoxy)-7-methoxyindan-2-yl]-4-bromo-2-[(N-carbo-2,2-dimethylethoxy)-amino]-7-methoxyindan-2-carboxamide [(*S,S*)-**17**]. To a solution of (*S*)-**9** (251 mg, 0.800 mmol), (*S*)-**11** (348 mg, 0.833 mmol), and triethylamine (232 μL) in DMF (3.2 mL) was added BOP reagent<sup>9</sup> (552 mg, 1.25 mmol). After stirring at room temperature for 60 h, the solution was diluted with EtOAc (30 mL) and water (30 mL). The organic layer was removed and the aqueous layer was extracted with EtOAc (2 x 30 mL). The organic extracts were combined and sequentially washed with 2 M HCl (3 x 30 mL), water (30 mL), saturated NaHCO<sub>3</sub> (3 x 30 mL), water (30 mL), then dried (MgSO<sub>4</sub>), filtered, and concentrated to give a light yellow solid, mp 203–204 °C. Flash chromatography (60% EtOAc/hexanes) afforded 432 mg (0.634 mmol, 79%) of (*S,S*)-**17**, [α]<sub>D</sub><sup>23</sup> +13 (c 0.72, CDCl<sub>3</sub>), R<sub>f</sub> 0.14 (20% EtOAc/hexanes), which was otherwise identical to racemic **17**.

Anal. Calcd for C<sub>29</sub>H<sub>34</sub>Br<sub>2</sub>N<sub>2</sub>O<sub>7</sub>: C, 51.04; H, 5.02; N, 4.11. Found: C, 51.08; H, 5.17; N, 4.02.

(*R,S*)-Cyclo-[phenylalanyl-(2-amino-4-bromo-7-methoxyindan-2-carboxylic acid)] [(*R,S*)-**4**]. A sample of (*R,S*)-**13** (98.7 mg, 0.176 mmol) was heated in a sealed, evacuated tube for 30 min at 245–250 °C in an oil bath. The sample melted, evolved gas and resolidified. After cooling to room temperature, the solid was recrystallized from DMSO to give 55 mg (0.13 mmol, 75%) of (*R,S*)-**4** as a white solid, mp > 290 °C (dec). [α]<sub>D</sub><sup>23</sup> +2.0 (c 0.83, CDCl<sub>3</sub>); IR cm<sup>-1</sup> 3180, 3059, 2960, 1672, 1450; <sup>1</sup>H NMR (DMSO-*d*<sub>6</sub>) δ 2.06 (1, d, J = 17.4 Hz), 2.43 (1, d, J = 17.7 Hz), 2.86–2.91 (2, m), 3.15 (1, m), 3.18 (1, m), 3.68 (3, s), 4.27 (1, m), 6.68 (1, d,

$J = 9.0$  Hz), 7.17–7.32 (6, m), 8.29 (1, m), 8.53 (1, m);  $^{13}\text{C}$  NMR (DMSO- $d_6$ )  $\delta$  38.4, 44.8, 48.2, 55.4, 55.7, 61.9, 108.3, 111.0, 126.8, 128.1, 129.3, 130.3, 130.4, 135.9, 141.5, 154.2, 165.8, 169.8.

Anal. Calcd for  $\text{C}_{20}\text{H}_{19}\text{BrN}_2\text{O}_3$ : C, 57.84; H, 4.61; N, 6.75. Found: C, 57.30; H, 4.46; N, 6.74.

*(S,S)*-Cyclo-[phenylalanyl-(2-amino-4-bromo-7-methoxyindan-2-carboxylic acid)] [(*S,S*)-4]. A sample of (*S,S*)-13 (53 mg, 0.094 mmol) was heated in a sealed, evacuated tube for 30 min at 245–250 °C in an oil bath. The sample melted, evolved gas, and resolidified. After cooling to room temperature, the solid was recrystallized from DMSO to give 29.8 mg (0.072 mmol, 77%) of (*S,S*)-4 as a white solid, mp 302–308 °C.  $[\alpha]_{\text{D}}^{23} -8.1$  ( $c$  0.44, TFA); IR  $\text{cm}^{-1}$  3180, 3044, 2957, 1672, 1450;  $^1\text{H}$  NMR (DMSO- $d_6$ )  $\delta$  1.88 (1, d,  $J = 17.7$  Hz), 2.22 (1, d,  $J = 17.1$  Hz), 2.84–2.90 (2, m), 3.16 (1, m), 3.38 (1, m), 3.70 (3, s), 4.27 (1, m), 6.69 (1, d,  $J = 8.7$  Hz), 7.17–7.32 (6, m), 8.30 (1, s), 8.51 (1, s);  $^{13}\text{C}$  NMR (DMSO- $d_6$ )  $\delta$  38.5, 44.5, 48.6, 55.3, 55.8, 61.8, 108.3, 111.0, 127.4, 128.2, 129.7, 130.3, 130.4, 135.6, 141.2, 154.2, 165.7, 169.8.

Anal. Calcd for  $\text{C}_{20}\text{H}_{19}\text{BrN}_2\text{O}_3$ : C, 57.84; H, 4.61; N, 6.75. Found: C, 57.42; H, 4.48; N, 6.62.

*(R,S)*-Cyclo-bis(2-amino-4-bromo-7-methoxyindan-2-carboxylic acid) (meso-5). A sample of (*R,S*)-17 (100 mg, 0.15 mmol) was heated in a sealed, evacuated tube for 30 min at 245–250 °C in an oil bath. The sample melted, evolved gas, and resolidified. After cooling to room temperature, the solid was recrystallized from DMSO to give 50 mg (0.093 mmol, 64%) of meso-5 as a white solid, mp 357–359 °C. IR  $\text{cm}^{-1}$  3175, 3043, 2957, 1678;  $^1\text{H}$  NMR (DMSO- $d_6$ )  $\delta$  3.13 (2, d,  $J = 16.8$  Hz), 3.15 (2, d,  $J = 16.8$  Hz), 3.53 (2, d,  $J = 16.8$  Hz), 3.57 (2, d,  $J = 16.5$  Hz), 3.77 (6, s), 6.80 (2, d, 8.7 Hz), 7.36 (2, d, 8.7 Hz), 8.82 (2, s);  $^{13}\text{C}$  NMR (DMSO- $d_6$ )  $\delta$  44.7, 48.1, 55.4, 62.7, 108.5, 111.3, 129.2, 130.7, 141.2, 154.5, 170.1.

Anal. Calcd for  $\text{C}_{22}\text{H}_{20}\text{Br}_2\text{N}_2\text{O}_4$ : C, 49.28; H, 3.76; N, 5.22. Found: C, 49.25; H, 3.60; N, 5.07.

*(±)*-Cyclo-bis(2-amino-4-bromo-7-methoxyindan-2-carboxylic acid) (*rac*-5). A 1:1 mixture of (*S,S*)-17 and (*R,R*)-17 (100 mg, 0.15 mmol) was heated in a sealed, evacuated tube for 30 min at 245–250 °C in an oil bath. The sample melted, evolved gas, and resolidified. After cooling to room temperature, the solid was recrystallized from DMSO to give 49 mg (0.091 mmol, 62%) of *rac*-5 as a white solid, mp 348–351 °C. IR  $\text{cm}^{-1}$  3175, 3043, 2955, 1681;  $^1\text{H}$  NMR (DMSO- $d_6$ )  $\delta$  3.14 (2, d,  $J = 16.8$  Hz), 3.15 (2, d,  $J = 16.8$  Hz), 3.54 (2, d,  $J = 16.8$  Hz), 3.57 (2, d,  $J = 16.8$  Hz), 3.78 (6, s), 6.80 (2, d, 9.0 Hz), 7.37 (2, d, 8.4 Hz), 8.82 (2, s);  $^{13}\text{C}$  NMR (DMSO- $d_6$ )  $\delta$  45.3, 47.4, 55.4, 62.7, 108.5, 111.2, 128.9, 130.8, 141.5, 154.5, 170.1.

Anal. Calcd for  $\text{C}_{22}\text{H}_{20}\text{Br}_2\text{N}_2\text{O}_4$ : C, 49.28; H, 3.76; N, 5.22. Found: C, 49.23; H, 3.77; N, 5.22.

*(S,S)*-Cyclo-bis(2-amino-4-bromo-7-methoxyindan-2-carboxylic acid) (*S,S*)-5. A sample of (*S,S*)-17 (100 mg, 0.15 mmol) was heated in a sealed, evacuated tube for 30 min at 245–250 °C in an oil bath. The sample melted, evolved gas, and resolidified. After cooling to room temperature, the solid was recrystallized from DMSO to give 49 mg (0.091 mmol, 62%) of (*S,S*)-5 as a white solid, mp 360–362 °C,  $[\alpha]_{\text{D}}^{23} -15$  ( $c$  0.39, TFA), which was otherwise identical to *rac*-5.

Anal. Calcd for  $\text{C}_{22}\text{H}_{20}\text{Br}_2\text{N}_2\text{O}_4$ : C, 49.28; H, 3.76; N, 5.22. Found: C, 48.98; H, 3.66; N, 5.27.

### ACKNOWLEDGMENT

Financial support of this research from Research Corporation, from the Office of Naval Research through the Center for Advanced Multifunctional Nonlinear Optical Polymers and Molecular Assemblies, and from the University of Arizona through the Materials Characterization Program and the Office of the Vice President for Research is gratefully acknowledged. Assistance from Dr. Michael Bruck and the staff of the Molecular Structure Lab at the University of Arizona Department of Chemistry, and from Dr. Victor G. Young, Jr., of the X-ray Crystallographic Laboratory at The University of Minnesota, is gratefully acknowledged.

### REFERENCES

1. (a) Lyon, S. R. Ph.D. Dissertation, The University of Arizona, Tucson, AZ, 1993. (b) Williams, L. J. Ph.D. Dissertation, The University of Arizona, Tucson, AZ, 1996. (c) Mash, E. A.; Williams, L. J. *Polym. Preprints* **1996**, *37*, 207.
2. Williams, L. J.; Jagadish, B.; Kloster, R. A.; Lyon, S. R.; Carducci, M. D.; Mash, E. A. *Tetrahedron*, preceding article in this issue.
3. For other crystal engineering efforts involving piperazine–2,5–diones, see: (a) Brienne, M–J.; Gabard, J.; Leclercq, M.; Lehn, J.–M.; Cesario, M.; Pascard, C.; Chev e, M.; Dutruc–Rosset, G. *Tetrahedron Lett.* **1994**, *35*, 8157–8160. (b) Palacin, S.; Chin, D. N.; Simanek, E. E.; MacDonald, J. C.; Whitesides, G. M.; McBride, M. T.; Palmore, G. T. R. *J. Am. Chem. Soc.* **1997**, *119*, 11807–11816. (c) Palmore, G. T. R.; McBride, M. T. *Chem. Commun.* **1998**, *119*, 145–146. (d) Chin, D. N.; Palmore, G. T. R.; Whitesides, G. M. *J. Am. Chem. Soc.* **1999**, *121*, 2115–2122.
4. (a) Desiraju, G. R. *Crystal Engineering: The Design of Organic Solids*; Elsevier: Amsterdam, 1989, p. 249. (b) Gavezzotti, A. *Acc. Chem. Res.* **1994**, *27*, 309–314. (c) Whitesell, J. K.; Davis, R. E.; Saunders, L. L.; Wilson, R. J.; Feagins, J. P. *J. Am. Chem. Soc.* **1991**, *113*, 3267–3270. (d) Gavezzotti, A. *J. Phys. Chem.* **1990**, *94*, 4319–4325.
5. Stork, G.; Leong, A. Y. W.; Touzin, A. M. *J. Org. Chem.* **1976**, *41*, 3491–3493.
6. (a) Goldberg, Y.; Bensimon, C.; Alper, H. *J. Org. Chem.* **1992**, *57*, 6374–6376. (b) Gruter, G.–J. M.; Akkerman, O. S.; Bickelhaupt, F. *J. Org. Chem.* **1994**, *59*, 4473–4481.
7. This follows the method of Kuki; see Kotha, S.; Kuki, A. *Tetrahedron Lett.* **1992**, *33*, 1565–1568.
8. Purchased from Aldrich Chemical Company.

9. Castro, B.; Dormoy, J.-R.; Dourtoglou, B.; Evin, G.; Selve, C.; Ziegler, J.-C. *Synthesis* **1976**, 751–752.
10. (a) Edman, P. *Acta Chem. Scand.* **1950**, *4*, 283–293. (b) Edman, P. *Acta Chem. Scand.* **1950**, *4*, 277–282.
11. Glusker, J. P.; Lewis, M. Rossi, M. *Crystal Structure Analysis for Chemists and Biologists*; VCH: New York, 1994; pp. 44–45. As pointed out by one referee, the term "isostructural" is preferred over "isomorphic" since it has not been demonstrated that these compounds form solid solutions.
12. IUPAC–IUB Commission on Biochemical Nomenclature, *Biochemistry* **1970**, *9*, 3471–3479.
13. Allen, F. H.; Kennard, O. *Chemical Design Automation News* **1993**, *8*, 31–37.
14. (a) Karlström, G.; Linse, P.; Wallqvist, A.; Jönsson, B. *J. Am. Chem. Soc.* **1983**, *105*, 3777–3782. (b) Burley, S. K.; Petsco, G. A. *J. Am. Chem. Soc.* **1986**, *108*, 7995–8001. (c) Jorgensen, W. L.; Severance, D. *J. Am. Chem. Soc.* **1990**, *112*, 4768–4774. (d) Hobza, P.; Selzle, H. L.; Schlag, E. W. *J. Am. Chem. Soc.* **1994**, *116*, 3500–3506.
15. Edge-to-face arene interactions are considered stabilizing (ref. 14), but the origin and magnitude of such interactions have recently come under scrutiny. See (a) Kim, E.; Paliwal, S.; Wilcox, C. S. *J. Am. Chem. Soc.* **1998**, *120*, 11192–11193 and references cited therein. (b) Umezawa, Y.; Tsuboyama, S.; Honda, K.; Uzawa, J.; Nishio, M. *Bull. Chem. Soc. Jpn.* **1998**, *71*, 1207–1213 and references cited therein.
16. (a) Gdaniec, M.; Liberek, B. *Acta Cryst.* **1986**, *C42*, 1343–1345. (b) Suguna, K.; Ramakumar, S.; Nagaraj, R.; Balaram, P. *Acta Cryst.* **1985**, *C41*, 284–286.
17. The bromine and methoxy groups are of comparable size; see Eliel, E. L.; Wilen, S. H.; Mander, L. N. *Stereochemistry of Organic Compounds*; John Wiley & Sons: New York, 1994, p. 696 and references cited therein.
18. Dunand, A.; Gerdil, R. *Acta Cryst.* **1984**, *B40*, 59–64.
19. Brock, C. P.; Dunitz, J. D. *Chem. Mater.* **1994**, *6*, 1118–1127; see footnote 57.
20. The molecular dipoles for (*R,S*)-**4** and (*S,S*)-**4**, calculated at the 3–21G(\*) level using MacSpartan v1.1, were 2.38 D and 2.07 D, respectively.
21. The molecular dipoles for meso-**5** and (*S,S*)-**5**, calculated at the 3–21G(\*) level using MacSpartan v1.1, were 0.00 D and 4.40 D, respectively.